

Article

LOS-Based Equal Gain Transmission and Combining in General Frequency-Selective Ricean Massive MIMO Channels

Qiuna Yan ^{1,2}, Yu Sun ¹ and Dian-Wu Yue ^{1,*} 

¹ School of Information Science and Technology, Dalian Maritime University, Dalian 116026, China; qiu7589@dlnu.edu.cn (Q.Y.); suny@dlnu.edu.cn (Y.S.)

² State Key Laboratory of Integrated Services Networks, Xidian University, Xi'an 710071, China

* Correspondence: dwyue@dlnu.edu.cn; Tel.: +86-411-8472-4261

Received: 13 December 2018; Accepted: 7 January 2019; Published: 10 January 2019

Abstract: In general frequency-selective Ricean fading environments with doubly-ended spatial correlation, this paper investigates the spectral efficiency of a broadband massive multiple-input multiple-output (MIMO) system. In particular, in order to reduce overhead of channel estimation effectively, it proposes a scheme of equal gain transmission and combining, which is only based on line-of-sight (LOS) component and has low hardware complexity. With the scheme, several interesting transmit power scaling properties without and with spatial correlation are derived when the number of antennas at the transmitter or the number of antennas at the receiver grows in an unlimited way. Furthermore, the asymptotical rate analysis is extended to the cooperative relaying scenarios with decode-and-forward and amplify-and-forward protocols, respectively, and then two novel power scaling laws are given.

Keywords: massive MIMO; beamforming; line-of-sight; Ricean fading; frequency-selective; power scaling

1. Introduction

Recently, massive multiple-input multiple-output (MIMO) has attracted great interest in both academia and industry, and has been a promising solution to meet the demanding spectral efficiency requirement of 5G systems [1]. Its promising benefits includes significant increase of both spectral and energy efficiencies [2–4]. Interestingly, the two benefits of massive MIMO can be achieved by maximum-ratio transmission/maximum-ratio combining (MRT/MRC) or zero-forcing (ZF) precoding/detection [3,5].

With MRT/MRC and ZF linear processing, many scholars have given various asymptotic performance analyses. In particular, the power scaling law in the limit of the large number of antennas has been widely studied in order to quantify the power savings. For Rayleigh and Ricean fading environments, with MRC and ZF detectors, authors in [3,6] analyzed uplink massive MIMO system performance. If perfect channel state information (CSI) is available, they showed that, when the number of base station (BS) antennas grows large and the transmit power of each user is scaled down proportionally to it, the ergodic achievable rate can asymptotically be equal to a positive constant.

In order to obtain the needed CSI, channel estimation must be obviously carried on [7]. However, the channel estimation will result in not only heavy overhead but also pilot contamination in multi-cells, which will become a serious problem [2,8]. For a point to point massive MIMO system in Ricean fading, to reduce the heavy overhead to estimate the CSI, we investigated a scheme with equal gain transmission /equal gain combining (EGT/EGC), which is only based on the line-of-sight (LOS) component (or say specular component) and has low hardware complexity [9]. It was showed that, with this scheme, the ergodic achievable rate can converge to that of the corresponding MRT/MRC

based on the perfect CSI as the two numbers of antennas at the transmitter and receiver go to infinity. After that, we further considered the novel linear processing scheme for a downlink or uplink multiuser massive MIMO system [10,11] and showed that each user in the downlink or uplink system can have asymptotically the same rate as in the single-user case when the number of BS antennas goes without bound.

It should be pointed out that the above-mentioned results with the novel scheme have only considered uncorrelated Ricean frequency-flat fading channels without a relay [12]. Recently, we tried to develop our analysis to frequency-selective Ricean fading channels [13], but only for a very simple and special scenario [14]. The EGT/EGC linear transmission scheme is very attractive for massive MIMO systems since it enables low-complexity and inexpensive hardware [15–18]. Motivated by these facts, in this paper, we make use of a comparatively complicated and general frequency-selective Ricean fading channel model [14,19,20] to investigate further the LOS-based EGT/EGC scheme. We firstly derive several interesting power scaling properties for broadband massive MIMO systems with and without spatial correlation. In particular, it is shown that the ergodic achievable rate of LOS-based EGT/EGC scheme can have the same asymptotic value as the ergodic achievable rate of the whole CSI-based MRT/MRC scheme if the two numbers of transmit and receive antennas go without bound and with a fixed ratio. Then, we extend our asymptotical performance analysis to the cooperative relaying scenarios with decode-and-forward (DF) protocol and with amplify-and-forward (AF) protocol, respectively, and obtain two novel power scaling laws for the two scenarios. In particular, it is also shown that the ergodic achievable rate of LOS-based scheme can have the same asymptotic value as the ergodic achievable rate of the CSI-based scheme if the number of source antennas and the two numbers of transmit and receive relay antennas go without bound and with two fixed ratios, respectively.

The manuscript is organized as follows: in Section 2, the system model is introduced. In Section 3, the proposed LOS-based transmission scheme is presented and its power scaling law without correlation and with correlation is derived, respectively. Extension of our analysis to a cooperative relaying system is given in Section 4. In Section 5, the analysis results are verified by simulation. Finally, in Section 6, some concluding remarks are given.

Notation: boldface lower and upper case letters denote column vectors and matrices, respectively. The superscripts $(\cdot)^\dagger$ and $(\cdot)^T$ stand for conjugate-transpose and transpose operations, respectively. The expectation operator is denoted by $\mathbb{E}\{\cdot\}$. $\alpha \sim \text{CN}(0, \delta^2)$ stands for a circularly symmetric complex Gaussian variable α which has zero mean and variance δ^2 .

2. System Model

Since a set of parallel independent frequency flat MIMO channels can be used to describe a frequency selective MIMO channel, we start with introducing the frequency flat channels [14,19].

For a point-to-point MIMO system over frequency-flat channels, we assume that it has N transmit antennas and M receive antennas. Then, we can represent a $M \times 1$ received signal vector as

$$\mathbf{y} = \sqrt{p}\mathbf{H}_0\mathbf{x} + \mathbf{z}, \quad (1)$$

where \mathbf{z} denotes the additive white Gaussian noise (AWGN) vector that has zero-mean and covariance matrix $\sigma^2\mathbf{I}_M$ with \mathbf{I}_M being the $M \times M$ identity matrix, \mathbf{x} denotes the transmitted signal vector, $\mathbf{H}_0 = [h_{mn}]_{m,n=1}^{M,N}$ stands for the $M \times N$ channel matrix whose element h_{mn} denotes the channel gain between the m -th antenna at the receiver and the n -th antenna at the transmitter, and p is the average transmitted power. The channel matrix \mathbf{H}_0 under Ricean fading consists of a LOS matrix and a scattered matrix, i.e.,

$$\mathbf{H}_0 = \sqrt{\bar{\kappa}_0} \bar{\mathbf{H}}_0 + \sqrt{\tilde{\kappa}_0} \tilde{\mathbf{H}}_0, \tag{2}$$

where $\bar{\kappa}_0 = \frac{\kappa_0}{1+\kappa_0}$, $\tilde{\kappa}_0 = \frac{1}{1+\kappa_0}$. Note that $\kappa_0 > 0$ represents the Ricean K -factor. The LOS matrix $\bar{\mathbf{H}}_0$ can be written as

$$\bar{\mathbf{H}}_0 = \mathbf{r}_0 \mathbf{t}_0^T. \tag{3}$$

Here, \mathbf{r}_0 denotes the specular array response at the receiver and can be expressed as

$$\mathbf{r}_0 = [1, e^{j2\pi d_r \sin(\theta)}, \dots, e^{j2\pi(M-1)d_r \sin(\theta)}]^T, \tag{4}$$

where θ is the angle of arrival of the LOS component and d_r is the antenna spacing normalized by wavelength at the receiver. Similarly, \mathbf{t}_0 denotes the specular array response at the transmitter and can be given by

$$\mathbf{t}_0 = [1, e^{j2\pi d_t \sin(\phi)}, \dots, e^{j2\pi(N-1)d_t \sin(\phi)}]^T \tag{5}$$

where ϕ is the angle of departure of the LOS component and d_t is the antenna spacing normalized by wavelength at the transmitter. The entries in the scattering matrix $\tilde{\mathbf{H}}_0$, $[\tilde{\mathbf{H}}_0]_{mn} \sim \text{CN}(0, 1)$, i.e., they are circular complex Gaussian random variables with zero mean and unit variance. Furthermore, we assume that they are independent and identically distributed (i.i.d).

Now, we are concerned with a broadband orthogonal frequency-division multiplexing (OFDM)-MIMO system with K subcarriers, where ideal OFDM transmission with proper cyclic prefix extension is assumed. For the k -th subcarrier, the input–output relationship is expressed as

$$\mathbf{y} = \sqrt{p} \mathbf{H} \mathbf{x} + \mathbf{z}, \tag{6}$$

where \mathbf{x} is just the normalized signal vector, \mathbf{z} is the AWGN vector, and \mathbf{H} is the channel matrix. The channel matrix can be given by as

$$\mathbf{H} = \sum_{\ell=0}^{L-1} \rho_\ell \mathbf{H}_\ell \exp(-j2\pi \frac{k}{K} \ell), \tag{7}$$

where L represents the channel delay spread, $\{\rho_\ell^2\}$ is the power delay profile satisfying $\sum_{\ell=0}^{L-1} \rho_\ell^2 = 1$, and \mathbf{H}_ℓ stands for the channel matrix at time delay ℓ . Furthermore, \mathbf{H}_ℓ , $\ell = 0, 1, \dots, L - 1$ are mutually uncorrelated, Ricean distributed, and can be expressed as in Label (2)

$$\mathbf{H}_\ell = \sqrt{\bar{\kappa}_\ell} \bar{\mathbf{H}}_\ell + \sqrt{\tilde{\kappa}_\ell} \tilde{\mathbf{H}}_\ell. \tag{8}$$

In particular, $\bar{\mathbf{H}}_\ell = \mathbf{r}_\ell \mathbf{t}_\ell^T$ is just as in Label (3) and $\tilde{\mathbf{H}}_\ell$ is also modeled as a random matrix consisting of i.i.d. elements.

3. LOS-Based EGT/EGC and Power Scaling Laws

3.1. The Scenario without Correlation

The scattered component of k -th subcarrier’s channel matrix can be described as

$$\tilde{\mathbf{H}} = \sum_{\ell=0}^{L-1} \rho_\ell \sqrt{\tilde{\kappa}_\ell} \tilde{\mathbf{H}}_\ell \exp(-j2\pi \frac{k}{K} \ell). \tag{9}$$

Now, it is assumed that $\tilde{\mathbf{H}}$ is not available, but the LOS component

$$\bar{\mathbf{H}} = \sum_{\ell=0}^{L-1} \rho_{\ell} \sqrt{\bar{\kappa}_{\ell}} \bar{\mathbf{H}}_{\ell} \exp(-j2\pi \frac{k}{K} \ell) \tag{10}$$

can be available. In what follows, by employing only $\bar{\mathbf{H}}$, we will present a linear processing scheme with EGT/EGC and then compare it with the MRT/MRC scheme based on the perfect CSI.

Since $\tilde{\mathbf{H}}$ is not available, a couple of the normalized weighting vectors \mathbf{w}_t and \mathbf{w}_r can be chosen in such a way that the effective output signal-to-noise ratio (SNR) can become maximum. The largest eigenvalue of matrix $\bar{\mathbf{H}}^{\dagger} \bar{\mathbf{H}}$ is now denoted by $\lambda_{\max}(\bar{\mathbf{H}}^{\dagger} \bar{\mathbf{H}})$. Due to the fact that $\mathbf{w}_r^{\dagger} \mathbf{z}^k \sim \text{CN}(0, \sigma^2)$, the effective output signal-to-interference-plus-noise ratio (SINR) can be described as

$$\gamma_S^{(k)} = \frac{p|\mathbf{w}_r^{\dagger} \bar{\mathbf{H}} \mathbf{w}_t^{\text{T}\dagger}|^2}{p|\mathbf{w}_r^{\dagger} \tilde{\mathbf{H}} \mathbf{w}_t^{\text{T}\dagger}|^2 + \sigma^2} = \frac{p\lambda_{\max}(\bar{\mathbf{H}}^{\dagger} \bar{\mathbf{H}})}{p|\mathbf{w}_r^{\dagger} \tilde{\mathbf{H}} \mathbf{w}_t^{\text{T}\dagger}|^2 + \sigma^2}. \tag{11}$$

We denote by R_S the ergodic achievable rate of the LOS-based scheme. Then,

$$R_S = \mathbb{E}\left\{\frac{1}{K} \sum_{k=0}^{K-1} \log_2(1 + \gamma_S^{(k)})\right\} = \frac{1}{K} \sum_{k=0}^{K-1} R_S^{(k)}, \tag{12}$$

where $R_S^{(k)} = \mathbb{E}\{\log_2(1 + \gamma_S^{(k)})\}$. We have the following results through the derivation.

Lemma 1. Define $\lambda_{\max}^{(k)} = \lambda_{\max}(\bar{\mathbf{H}}^{\dagger} \bar{\mathbf{H}})$ and $\bar{\kappa}_S = \sum_{\ell=0}^{L-1} \rho_{\ell}^2 \bar{\kappa}_{\ell}$. Then,

$$\log_2\left(1 + \frac{p\lambda_{\max}^{(k)}}{p\bar{\kappa}_S + \sigma^2}\right) \leq R_S^{(k)} \leq \log_2\left(1 + \frac{p\lambda_{\max}^{(k)}}{\sigma^2}\right). \tag{13}$$

Proof of Lemma 1. Regarding the ergodic achievable rate of the k -th subcarrier, it is easy for us to derive its following lower bound with the help of the well-known Jensen’s inequality:

$$R_S^{(k)} \geq \log_2\left(1 + \frac{1}{\mathbb{E}(1/\gamma_S^{(k)})}\right) = \log_2\left(1 + \frac{p\lambda_{\max}^{(k)}}{p \sum_{\ell=0}^{L-1} \rho_{\ell}^2 \mathbb{E}_{\ell} + \sigma^2}\right), \tag{14}$$

where $\mathbb{E}_{\ell} = \mathbb{E}|\mathbf{w}_r^{\dagger} \tilde{\mathbf{H}}_{\ell} \mathbf{w}_t^{\text{T}\dagger}|^2 = \bar{\kappa}_{\ell}$ for $0 \leq \ell \leq L - 1$. Thus,

$$R_S^{(k)} \geq \log_2\left(1 + \frac{p\lambda_{\max}^{(k)}}{p\bar{\kappa}_S + \sigma^2}\right). \tag{15}$$

Moreover, we can obtain from Label (11) that

$$R_S^{(k)} = \mathbb{E} \log_2\left(1 + \frac{p\lambda_{\max}^{(k)}}{p|\mathbf{w}_r^{\dagger} \tilde{\mathbf{H}} \mathbf{w}_t^{\text{T}\dagger}|^2 + \sigma^2}\right) \leq \log_2\left(1 + \frac{p\lambda_{\max}^{(k)}}{\sigma^2}\right). \tag{16}$$

Thus, Lemma 1 holds. \square

Lemma 2. Let $\bar{\kappa}_U = \sum_{\ell=0}^{L-1} \rho_{\ell}^2 \bar{\kappa}_{\ell}$. and $\bar{\kappa}_L = \max\{\rho_{\ell}^2 \bar{\kappa}_{\ell}, 0 \leq \ell \leq L - 1\}$. Then,

$$\bar{\kappa}_L \leq \lim_{MN \rightarrow \infty} \frac{\lambda_{\max}^{(k)}}{MN} \leq \bar{\kappa}_U. \tag{17}$$

Proof of Lemma 2. For $0 \leq \ell \leq L - 1$ and $0 \leq b \leq L - 1$, we define $\varphi_{\ell b} = 2\pi d_r(\sin(\theta_b) - \sin(\theta_{\ell}))$, and then have that

$$\frac{\bar{\mathbf{H}}_\ell^\dagger \bar{\mathbf{H}}_b}{MN} = \varrho_{\ell b} \mathbf{U}_{\ell b}, \tag{18}$$

where

$$\varrho_{\ell b} = \frac{\mathbf{r}_\ell^\dagger \mathbf{r}_b}{M} = \begin{cases} 1, & \text{for } \ell = b; \\ \frac{1 - e^{jM\varphi_{\ell b}}}{M(1 - e^{j\varphi_{\ell b}})}, & \text{for } \ell \neq b \end{cases} \tag{19}$$

and

$$\mathbf{U}_{\ell b} = \frac{\mathbf{t}_\ell^{\text{T}\dagger} \mathbf{t}_b^{\text{T}}}{N} = [u_{an}]_{a,n=1}^{N,N} \tag{20}$$

with $u_{an} = \frac{1}{N} e^{2\pi d_i((a-1)\sin(\theta_b) - (n-1)\sin(\theta_\ell))}$. Now, suppose that $M \geq N$. Noting that $\lim_{M \rightarrow \infty} \varrho_{\ell b} = 0$ for $\ell \neq b$ and $\text{tr}(\mathbf{U}_{\ell\ell}) = 1$, we can obtain that

$$\lim_{MN \rightarrow \infty} \frac{\lambda_{\max}(\bar{\mathbf{H}}^\dagger \bar{\mathbf{H}})}{MN} \leq \sum_{\ell=0}^{L-1} \rho_\ell^2 \bar{\kappa}_\ell \lim_{MN \rightarrow \infty} \lambda_{\max}\left(\frac{\bar{\mathbf{H}}_\ell^\dagger \bar{\mathbf{H}}_\ell}{MN}\right) = \bar{\kappa}_U. \tag{21}$$

Moreover, we also have

$$\lim_{MN \rightarrow \infty} \frac{\lambda_{\max}(\bar{\mathbf{H}}^\dagger \bar{\mathbf{H}})}{MN} \geq \bar{\kappa}_L \tag{22}$$

since, for any ℓ , we can get when $\mathbf{w}_t = \frac{\mathbf{t}_\ell}{\sqrt{N}}$ and $\mathbf{w}_r = \frac{\mathbf{r}_\ell}{\sqrt{M}}$

$$\lim_{MN \rightarrow \infty} \frac{\lambda_{\max}(\bar{\mathbf{H}}^\dagger \bar{\mathbf{H}})}{MN} \geq \lim_{MN \rightarrow \infty} \frac{|\mathbf{w}_r^\dagger \tilde{\mathbf{H}} \mathbf{w}_t^{\text{T}\dagger}|^2}{MN} = \bar{\kappa}_\ell. \tag{23}$$

Therefore, Lemma 2 holds when $M \geq N$. When $N \geq M$, we can also similarly prove that Lemma 2 holds, based on the fact that $\lambda_{\max}(\bar{\mathbf{H}}^\dagger \bar{\mathbf{H}}) = \lambda_{\max}(\bar{\mathbf{H}} \bar{\mathbf{H}}^\dagger)$. \square

Proposition 1. *If $E = MNp$ be fixed as $MN \rightarrow \infty$, then we have*

$$\log_2\left(1 + \frac{E\bar{\kappa}_L}{\sigma^2}\right) \leq \lim_{MN \rightarrow \infty} R_S \leq \log_2\left(1 + \frac{E\bar{\kappa}_U}{\sigma^2}\right). \tag{24}$$

Proof of Proposition 1. If $E = MNp$ is fixed when $MN \rightarrow \infty$, we readily show that Proposition 1 holds by using Lemmas 1 and 2. \square

Remark 1. *This proposition gives the lower and upper bounds of the ergodic achievable rate of the LOS-based scheme. In the following special cases, we can obtain further the exact expressions of the ergodic achievable rate.*

Corollary 1. *When $N = 1$, we have, if $E = Mp$ be fixed as $M \rightarrow \infty$,*

$$\lim_{M \rightarrow \infty} R_S = \log_2\left(1 + \frac{E\bar{\kappa}_U}{\sigma^2}\right). \tag{25}$$

Similarly, when $M = 1$, we also have if $E = Np$ be fixed as $N \rightarrow \infty$

$$\lim_{N \rightarrow \infty} R_S = \log_2\left(1 + \frac{E\bar{\kappa}_U}{\sigma^2}\right). \tag{26}$$

Proof of Corollary 1. When $M = 1$ or $N = 1$, due to the fact that $\lim_{MN \rightarrow \infty} \frac{\lambda_{\max}(\bar{\mathbf{H}}^\dagger \bar{\mathbf{H}})}{MN} = \bar{\kappa}_U$, it easily follows that $\lim_{MN \rightarrow \infty} R_S = \log_2\left(1 + \frac{E\bar{\kappa}_U}{\sigma^2}\right)$. \square

Corollary 2. If $E = MNp$ be fixed as $M \rightarrow \infty$ and $N \rightarrow \infty$, then we have

$$\lim_{M,N \rightarrow \infty} R_S = \log_2\left(1 + \frac{E\bar{\kappa}_L}{\sigma^2}\right). \tag{27}$$

Proof of Corollary 2. Without loss of generality, $\bar{\mathbf{H}}$ can be rewritten as

$$\bar{\mathbf{H}} = \sum_{\ell=0}^{L-1} \rho_\ell \sqrt{\bar{\kappa}_\ell} \mathbf{r}_\ell \mathbf{t}_\ell^T \exp(-j2\pi \frac{k}{K} \ell), \tag{28}$$

where $\rho_0 \sqrt{\bar{\kappa}_0} \geq \rho_1 \sqrt{\bar{\kappa}_1} \geq \dots \geq \rho_{L-1} \sqrt{\bar{\kappa}_{L-1}}$. We can rewrite $\bar{\mathbf{H}}$ in a matrix form as

$$\bar{\mathbf{H}} = \mathbf{A}_r \mathbf{D} \mathbf{A}_t^T, \tag{29}$$

where \mathbf{D} is a $L \times L$ diagonal matrix, $[\mathbf{D}]_{ll} = \rho_\ell \sqrt{MN\bar{\kappa}_\ell}$, and \mathbf{A}_r and \mathbf{A}_t are defined as follows:

$$\mathbf{A}_r = \frac{1}{\sqrt{M}} [\mathbf{r}_0, \mathbf{r}_1, \dots, \mathbf{r}_{L-1}] \tag{30}$$

and

$$\mathbf{A}_t = \frac{1}{\sqrt{N}} [\mathbf{t}_0, \mathbf{t}_1 \exp(-j2\pi \frac{k}{K}), \dots, \mathbf{t}_{L-1} \exp(-j2\pi \frac{k}{K} (L-1))]. \tag{31}$$

Since both $\{\mathbf{r}_0, \mathbf{r}_1, \dots, \mathbf{r}_{L-1}\}$ and $\{\mathbf{t}_0, \mathbf{t}_1, \dots, \mathbf{t}_{L-1}\}$ are orthogonal vector sets when $M \rightarrow \infty$ and $N \rightarrow \infty$ [21], \mathbf{A}_r and \mathbf{A}_t are asymptotically unitary matrices. For matrix $\bar{\mathbf{H}}$, thus we can form a singular value decomposition (SVD) as follows

$$\bar{\mathbf{H}} = \mathbf{U} \mathbf{\Sigma} \mathbf{V}^T = [\mathbf{A}_r | \mathbf{A}_r^\perp] \mathbf{\Sigma} [\mathbf{A}_t | \mathbf{A}_t^\perp]^T, \tag{32}$$

where $\mathbf{\Sigma}$ is a diagonal matrix including all singular values on its diagonal, i.e.,

$$[\mathbf{\Sigma}]_{ll} = \begin{cases} \rho_\ell \sqrt{MN\bar{\kappa}_\ell}, & \text{for } 0 \leq l \leq L-1, \\ 0, & \text{for } l > L-1. \end{cases} \tag{33}$$

Then,

$$\lim_{M,N \rightarrow \infty} \frac{\lambda_{\max}^{(k)}}{MN} = \rho_0^2 \bar{\kappa}_0 = \bar{\kappa}_L. \tag{34}$$

Thus, we finally obtain the desired result. \square

On the other hand, suppose that the perfect CSI is known, i.e., both of the LOS and scattered components are available at the transmitter and the receiver. Then, the weighting vectors \mathbf{w}_t and \mathbf{w}_r should be chosen in such a way that the exact output SNR is maximized. Thus, the resulting output SNR can be written as [11]

$$\gamma_P^{(k)} = \frac{p}{\sigma^2} \lambda_{\max}(\mathbf{H}^\dagger \mathbf{H}), \tag{35}$$

where $\lambda_{\max}(\mathbf{H}^\dagger \mathbf{H})$ stands for the largest eigenvalue of $\mathbf{H}^\dagger \mathbf{H}$. For the MRT/MRC scheme based on the perfect CSI, let R_P represent its ergodic achievable rate, i.e., $R_P = \mathbb{E}\{\frac{1}{K} \sum_{k=0}^{K-1} \log_2(1 + \gamma_P^{(k)})\}$. Now, we obtain the following power scaling law.

Proposition 2. When $M \rightarrow \infty$ and $N \rightarrow \infty$, suppose that $E = MNp$ is fixed and $N/M \rightarrow \mu$. We have that

$$\lim_{M,N \rightarrow \infty} R_P = \lim_{M,N \rightarrow \infty} R_S. \tag{36}$$

Proof of Proposition 2. Due to the fact $\mathbf{H} = \bar{\mathbf{H}} + \tilde{\mathbf{H}}$, we can have

$$\begin{aligned} \frac{1}{M}[\mathbf{H}^\dagger \mathbf{H}] &= \frac{1}{M}[(\bar{\mathbf{H}} + \tilde{\mathbf{H}})^\dagger (\bar{\mathbf{H}} + \tilde{\mathbf{H}})] \\ &= \frac{\bar{\mathbf{H}}^\dagger \bar{\mathbf{H}}}{M} + \frac{\bar{\mathbf{H}}^\dagger \tilde{\mathbf{H}}}{M} + \frac{\tilde{\mathbf{H}}^\dagger \bar{\mathbf{H}}}{M} + \frac{\tilde{\mathbf{H}}^\dagger \tilde{\mathbf{H}}}{M}. \end{aligned} \tag{37}$$

If we let

$$\mathbf{G} = \frac{\bar{\mathbf{H}}^\dagger \tilde{\mathbf{H}}}{M} = [g_{uv}]_{u,v=1}^{N,N}, \tag{38}$$

it follows that

$$g_{uv} = \frac{1}{M} \sum_{k=1}^M [\bar{\mathbf{H}}^\dagger]_{uk} [\tilde{\mathbf{H}}]_{kv}. \tag{39}$$

With the aid of (9) and (10), we can have that $|\bar{\mathbf{H}}^\dagger]_{uk}|^2 \leq \bar{\kappa}_S \leq 1$, and $[\tilde{\mathbf{H}}]_{kv} \sim \text{CN}(0, \delta^2)$ with $\delta^2 = \bar{\kappa}_S \leq 1$. As $[\tilde{\mathbf{H}}]_{kv}, 1 \leq k \leq M$ are independent each other, we know that

$$g_{uv} \sim \text{CN}(0, \sigma_{uv}^2), \quad \sigma_{uv}^2 \leq \frac{1}{M}. \tag{40}$$

Thus, it can follow that, when $M \rightarrow \infty, \mathbf{G} \rightarrow \mathbf{Q}$, where \mathbf{Q} denotes a matrix with all zero elements. Similarly, we can have that, if $M \rightarrow \infty$,

$$\mathbf{G}^\dagger = \frac{\tilde{\mathbf{H}}^\dagger \bar{\mathbf{H}}}{M} \rightarrow \mathbf{Q}. \tag{41}$$

Now, M is assumed to be large enough. Then, we certainly have that

$$\begin{aligned} \lambda_{\max}\left(\frac{\mathbf{H}^\dagger \mathbf{H}}{M}\right) &= \lambda_{\max}\left(\frac{\bar{\mathbf{H}}^\dagger \bar{\mathbf{H}}}{M} + \frac{\tilde{\mathbf{H}}^\dagger \tilde{\mathbf{H}}}{M}\right) \\ &\leq \lambda_{\max}\left(\frac{\bar{\mathbf{H}}^\dagger \bar{\mathbf{H}}}{M}\right) + \lambda_{\max}\left(\frac{\tilde{\mathbf{H}}^\dagger \tilde{\mathbf{H}}}{M}\right). \end{aligned} \tag{42}$$

When $M \rightarrow \infty$, suppose that $N/M \rightarrow \mu$. Then, we easily derive from ([22], Theorem 2.37), only noting that $[\tilde{\mathbf{H}}]_{mn} \sim \text{CN}(0, \bar{\kappa}_S)$

$$\lambda_{\max}\left(\frac{1}{M} \tilde{\mathbf{H}}^\dagger \tilde{\mathbf{H}}\right) \rightarrow \bar{\kappa}_S (1 + \sqrt{\mu})^2. \tag{43}$$

Thus, we further get

$$\lambda_{\max}\left(\frac{1}{MN} \mathbf{H}^\dagger \mathbf{H}\right) \leq \lambda_{\max}\left(\frac{1}{MN} \bar{\mathbf{H}}^\dagger \bar{\mathbf{H}}\right) + \bar{\kappa}_S (1 + \sqrt{\mu})^2 / N. \tag{44}$$

In addition, we can obtain

$$\lambda_{\max}\left(\frac{1}{MN} \mathbf{H}^\dagger \mathbf{H}\right) \geq \lambda_{\max}\left(\frac{1}{MN} \bar{\mathbf{H}}^\dagger \bar{\mathbf{H}}\right). \tag{45}$$

When $M \rightarrow \infty$ and $N \rightarrow \infty$, we can get, by combining (44) with (45),

$$\lambda_{\max}\left(\frac{1}{MN} \mathbf{H}^\dagger \mathbf{H}\right) \rightarrow \lim_{M,N \rightarrow \infty} \frac{\lambda_{\max}^{(k)}}{MN}. \tag{46}$$

It should be noticed that

$$\begin{aligned}
 R_P &= \frac{1}{K} \sum_{k=1}^K \mathbb{E} \log_2 \left(1 + \frac{p}{\sigma^2} \lambda_{\max}(\mathbf{H}^\dagger(k)\mathbf{H}(k)) \right) \\
 &= \frac{1}{K} \sum_{k=1}^K \mathbb{E} \log_2 \left(1 + \frac{pMN}{\sigma^2} \lambda_{\max} \left(\frac{\mathbf{H}^\dagger(k)\mathbf{H}(k)}{MN} \right) \right).
 \end{aligned} \tag{47}$$

Therefore, when $M \rightarrow \infty$ and $N \rightarrow \infty$, if $E = pMN$ is fixed, we can have finally

$$\lim_{M,N \rightarrow \infty} R_P = \lim_{M,N \rightarrow \infty} R_S. \tag{48}$$

Thus, Proposition 2 holds. \square

Remark 2. This proposition implies that, when the two numbers of antennas at the transmitter and the receiver grow large with a fixed ratio, the ergodic achievable rate of the LOS-based scheme has the same asymptotic value as the ergodic achievable rate of the whole CSI-based scheme.

3.2. The Scenario with Correlation

Now, we consider extending the proposed LOS-based ECT/EGC without spatial correlation to the scenario in which there exists doubly-ended spatial correlation. The MIMO system model presented in Section 2 is necessarily modified. $\tilde{\mathbf{H}}_\ell, \ell = 0, 1, 2, \dots, L - 1$ is now modeled as doubly-correlated Rayleigh fading, with transmit and receive correlation matrices Ψ_ℓ and Φ_ℓ , i.e., [12],

$$\tilde{\mathbf{H}}_\ell = [\Phi_\ell]^{1/2} \tilde{\mathbf{H}}_\ell^\omega [\Psi_\ell]^{1/2}, \tag{49}$$

where $\tilde{\mathbf{H}}_\ell^\omega$ is an i.i.d. matrix with each entry $\sim \text{CN}(0, 1)$. Since the scattered component of the channel matrix remains unchanged, the needed weighting vectors \mathbf{w}_t and \mathbf{w}_r should also remain unchanged. The ergodic achievable rate of the scenario with spatial correlation is denoted by

$$R_C = \frac{1}{K} \sum_{k=0}^{K-1} R_C^{(k)}, \quad R_C^{(k)} = \mathbb{E} \{ \log_2(1 + \gamma_C^{(k)}) \}. \tag{50}$$

With respect to R_C , we have the following results by a similar derivation.

Lemma 3.

$$\log_2 \left(1 + \frac{p\lambda_{\max}^{(k)}}{p\tilde{\kappa}_C + \sigma^2} \right) \leq R_C^{(k)} \leq \log_2 \left(1 + \frac{p\lambda_{\max}^{(k)}}{\sigma^2} \right), \tag{51}$$

where $\tilde{\kappa}_C = \sum_{\ell=0}^{L-1} \rho_\ell^2 \tilde{\kappa}_\ell \|\mathbf{w}_r^\dagger [\Phi_\ell]^{1/2}\|^2 \|[\Psi_\ell]^{1/2} \mathbf{w}_t^\dagger\|^2$.

Proposition 3. If $E = MNp$ is fixed as $MN \rightarrow \infty$, then

$$\lim_{MN \rightarrow \infty} R_C = \lim_{MN \rightarrow \infty} R_S. \tag{52}$$

Remark 3. This proposition implies that the two ergodic achievable rates with and without spatial correlation have the same asymptotic value when MN goes without bound.

4. Cooperative Relaying Systems

4.1. The Scenario with Decode-and-Forward Protocol

Ricean fading often happens in cooperative MIMO systems [23]. Therefore, we can use a Ricean MIMO channel model to describe both the source-relay and relay-destination links. Still in

frequency-selective Ricean fading environments, we especially study a classical cooperative relay system with a source node, a destination node and a relay node. The relay node can be equipped with a large-scale antenna array while both the source node and the destination node can be also equipped with a large-scale antenna array. The cooperative system with the three nodes is assumed to operate in a half-duplex mode, and the relay node employs the DF protocol for transmission. Each transmission for the system can be completed through two stages. Obviously, the cooperative system is a composite of two massive MIMO subsystems: one subsystem working at the first stage and the other subsystem at the second stage. Therefore, the rate analysis results mentioned above can be applied to the cooperative relay system.

We suppose that the relay makes use of M antennas to receive and transmit data and also suppose that the source has N_1 antennas and the destination has N_2 antennas. We denote the average transmitted power at the source and the relay by p_1 and p_2 , respectively. In addition, we still let R_P and R_S represent the ergodic achievable rates for the whole CSI-based MRT/MRC scheme and the LOS-based EGT/EGC scheme, respectively. Then, we can obtain the following power scaling property for the cooperative system.

Proposition 4. *When $M \rightarrow \infty$ and $N_1 \rightarrow \infty$, let $E_1 = MN_1p_1$ be fixed and $N_1/M \rightarrow \mu_1$ for the source-relay link. When $M \rightarrow \infty$ and $N_2 \rightarrow \infty$, let $E_2 = MN_2p_2$ be fixed and $N_2/M \rightarrow \mu_2$ for the relay-destination link. Then,*

$$\lim_{M, N_1, N_2 \rightarrow \infty} R_P = \lim_{M, N_1, N_2 \rightarrow \infty} R_S. \tag{53}$$

Proof of Proposition 4. From [24], it follows that the ergodic achievable rate with the perfect SCI-based MRT/MRC is written as

$$R_P = \min\{R_P^{(1)}/2, R_P^{(2)}/2\}, \tag{54}$$

where $R_P^{(1)}$ and $R_P^{(2)}$ are the corresponding ergodic achievable rates of the source-relay and relay-destination transmission links, respectively. Similarly, we also have that the ergodic achievable rate with the only LOS-based EGT/EGC can be given by

$$R_S = \min\{R_S^{(1)}/2, R_S^{(2)}/2\}, \tag{55}$$

where $R_S^{(1)}$ and $R_S^{(2)}$ are the corresponding ergodic achievable rates of the source-relay and relay-destination transmission links, respectively. Under the condition of Proposition 4, we get by Proposition 2

$$\lim_{M, N_1 \rightarrow \infty} R_P^{(1)} = \lim_{M, N_1 \rightarrow \infty} R_S^{(1)} \tag{56}$$

and

$$\lim_{M, N_2 \rightarrow \infty} R_P^{(2)} = \lim_{M, N_2 \rightarrow \infty} R_S^{(2)}. \tag{57}$$

Thus, it is easy to obtain the desired result (53). \square

Remark 4. *This proposition implies that, when the number of source antennas and the two numbers of relay antennas at the transmitter and the receiver grow large with fixed ratios, the ergodic achievable rate of the LOS-based scheme also has the same asymptotic value as the ergodic achievable rate of the whole CSI-based scheme.*

4.2. The Scenario with Amplify-and-Forward Protocol

The DF is a regenerative relaying transmission strategy. Now, we consider employing a nonregenerative strategy involving AF to replace the DF. Then, we can have a power scaling law as follows.

Proposition 5. Suppose that $N_1 = N_2 = 1$. When $M \rightarrow \infty$, let $E_1 = Mp_1$ and $E_2 = MN_2p_2$ be fixed. Then,

$$\lim_{M \rightarrow \infty} R_S = \log_2\left(1 + \left(\frac{E_1 \bar{\kappa}_{U1}}{\sigma_1^2} \cdot \frac{E_2 \bar{\kappa}_{U2}}{\sigma_2^2}\right) / \left(\frac{E_1 \bar{\kappa}_{U1}}{\sigma_1^2} + \frac{E_2 \bar{\kappa}_{U2}}{\sigma_2^2} + 1\right)\right). \quad (58)$$

Proof of Proposition 5. We denote by $\gamma_{S1}^{(k)}$ and $\gamma_{S2}^{(k)}$ the output instantaneous SNR of the source-relay and relay-destination links, respectively. From [25], we obtain that

$$\begin{aligned} R_S &= \frac{1}{K} \sum_{k=0}^{K-1} \mathbb{E}\{\log_2(1 + \gamma_S^{(k)})\} \\ &= \frac{1}{K} \sum_{k=0}^{K-1} \mathbb{E}\{\log_2(1 + (\gamma_{S1}^{(k)} \cdot \gamma_{S2}^{(k)}) / (\gamma_{S1}^{(k)} + \gamma_{S2}^{(k)} + 1))\}. \end{aligned} \quad (59)$$

Based on the proof of Lemma 2, we can have the following asymptotical SNR expressions

$$\lim_{M \rightarrow \infty} \gamma_{S1}^{(k)} = \frac{E_1 \bar{\kappa}_{U1}}{\sigma_1^2} \quad (60)$$

and

$$\lim_{M \rightarrow \infty} \gamma_{S2}^{(k)} = \frac{E_1 \bar{\kappa}_{U2}}{\sigma_2^2} \quad (61)$$

Thus, the power scaling law (58) holds. \square

5. Simulation Results

For OFDM-MIMO systems in frequency-selective Ricean fading channels, we in this section provide our analytical results and simulation results. In all simulations, we assume that all of these spacings between adjacent antennas at the transmitter and the receiver are 0.5. We set the number of subcarriers $K = 256$, the channel delay spread $L = 3$, and the noise variance as $\sigma^2 = 1$. In addition, we let $\rho_0^2 = \rho_1^2 = \rho_2^2 = 1/3$, $\theta_0 = \phi_0 = \pi/6$, $\theta_1 = \phi_1 = \pi/4$, and $\theta_2 = \phi_2 = \pi/3$. In Figures 1 and 2, the Ricean K-factor κ is fixed and is equal to 5 dB.

In order to verify Propositions 1 and 3, we consider firstly the scenario with spatial correlation when $N = 3$ and $E = 20$ dB. The spatial correlation among antennas is assumed to follow the exponential model, i.e., the correlation magnitude between antenna p and q can be determined by $c(p, q) = g^{|p-q|}$, where g denotes the correlation coefficient [12]. Therefore, we represent the correlation matrices (i, j) -th of Φ_ℓ by $[\Phi_\ell]_{ij} = (g_r^\ell)^{|i-j|}$ and (i, j) -th of Ψ_ℓ by $[\Psi_\ell]_{ij} = (g_t^\ell)^{|i-j|}$, respectively, $\ell = 0, 1, 2$. Moreover, we set $g_r^0 = g_r^1 = g_r^2 = g_r$ and $g_t^0 = g_t^1 = g_t^2 = g_t$. For the correlation coefficients $g_t = g_r = g = 0, 0.3, 0.6, 0.9$, as M increases from 6 to 60, Figure 1 provides a curve of the exact average rate R_C and two curves of the upper and lower bounds of R_S . It can be observed that the exact ergodic rate R_C increases as the number of receive antenna M grows large, and is always between the two bounds of R_S . As both of the correlation coefficients (g_t, g_r) increase, R_C is closer to the upper bound, and becomes higher and higher than R_S . This indicates that, compared to the uncorrelated scenario, the presence of spatial correlation results in improving the rate performance under the LOS-based EGT/EGC scheme. Therefore, if the LOS-based scheme can be employed, we can achieve performance benefits from the spatial correlation, which is obviously different from the traditional point of view. This implies that it would be practical if a large-scale antenna array is compactly arranged.

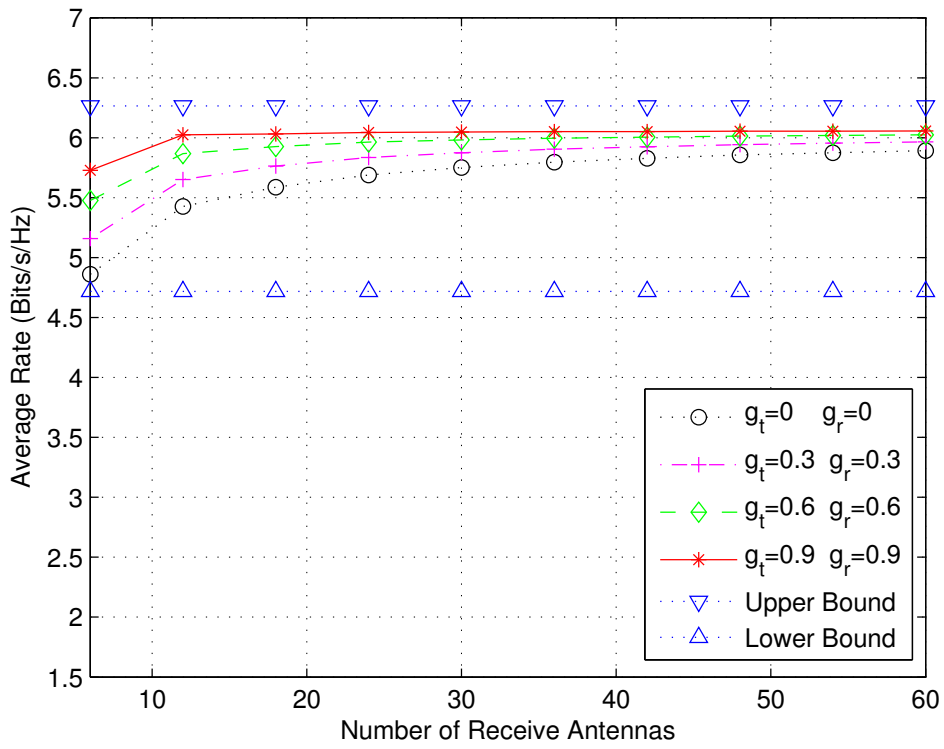


Figure 1. The ergodic achievable rate versus the number of receive antennas for comparing the case with correlation and the case without correlation.

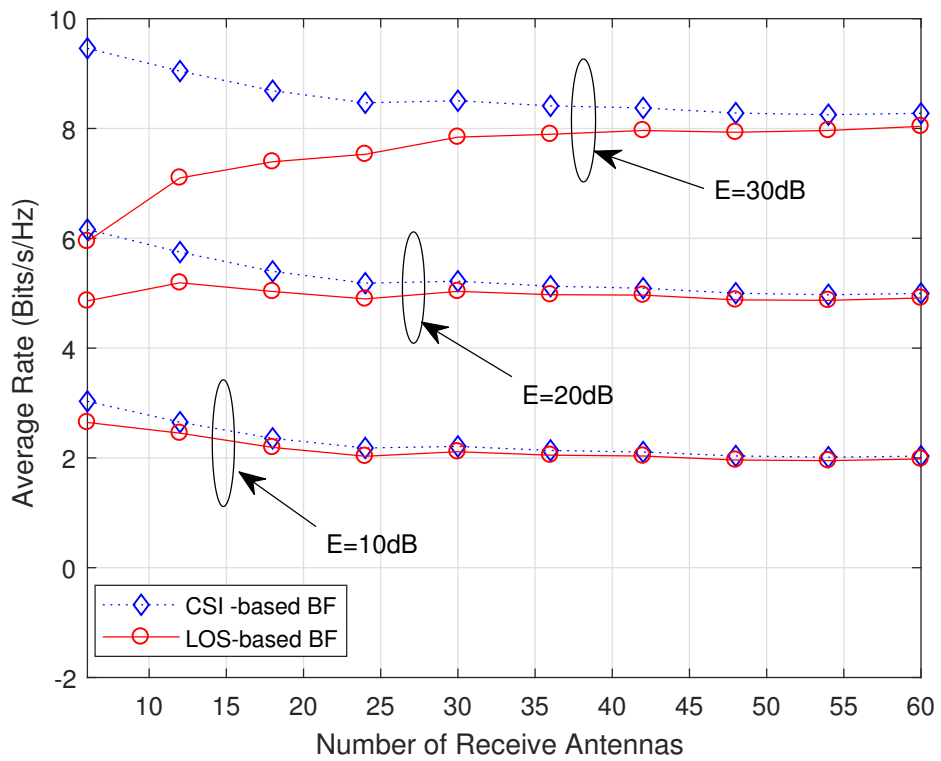


Figure 2. The ergodic achievable rate versus the number of receive antennas for comparing the LOS-based scheme with the whole CSI-based scheme.

Next, we consider validating Proposition 2. For that, we need to compare the ergodic achievable rate of the proposed LOS-based EGT/EGC scheme with that of the perfect CSI-based MRT/MRC scheme. We set $\mu = 1/2$ when the numbers of antennas at the transmitter and receiver grow large. For the parameter $E = 10, 20, 30$ dB, as M increases from 6 to 60, Figure 2 plots the two ergodic achievable rates, R_S and R_P . It can be found from Figure 2 that both of the ergodic achievable rates can tend to the same limit results for the given values of E . However, with an increase of E , the speed of rate convergence appears to be slower and slower.

Finally, we pay our attention to the classical DF cooperative relay system consisting of the source-relay and relay-destination links and set the identical parameters mentioned above in the two links. When $N_1 = N_2 = 6$, as M increases from 6 to 60, Figure 3 plots the two average rates R_S and R_P for $\kappa = 5, 15$ dB. It can be found from Figure 3 that, with an increasing κ , both R_S and R_P improve and R_S is closer to R_P . It should be noticed that R_P denotes the average rate for the traditional linear processing scheme based on the whole CSI as considered in [6]. For obtaining a comprehensive comparison with the scheme based on the whole CSI in Rayleigh fading discussed in [24], Figure 3 also includes a rate curve which corresponds to $\kappa = -\infty$ dB. Interestingly, with $\kappa = 5$ dB, the LOS-based scheme always obviously outperforms the scheme based on the whole CSI in Rayleigh fading.

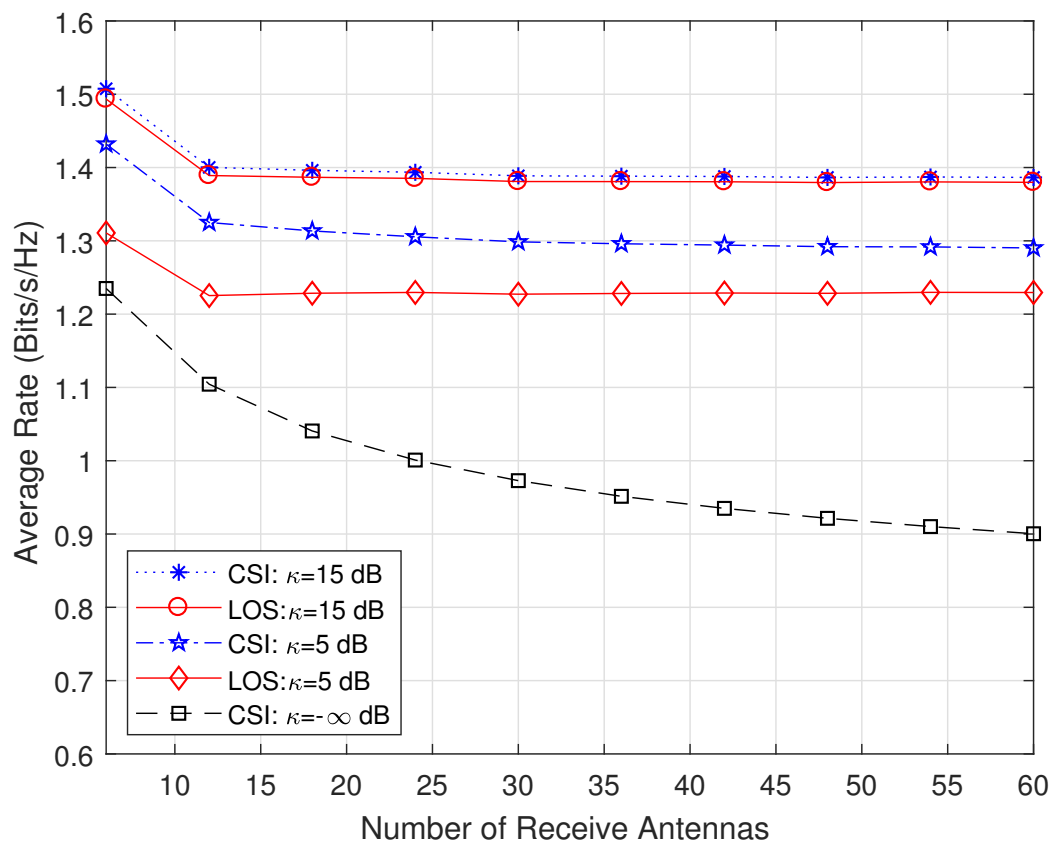


Figure 3. The ergodic achievable rate versus the number of relay antennas for comparing the case with Ricean fading and the case with Rayleigh fading.

6. Conclusions

In this paper, we have developed the transmission scheme of LOS-based EGT/EGC for point-to-point massive-MIMO systems in frequency-selective Ricean fading channels without and with spatial correlation. In particular, we have derived expressions of the system achievable rate and determined several power scaling laws. In addition, we have also generalized our analysis to the

cooperative relaying scenarios with DF and AF protocols, respectively. It is shown by our simulation results that the spatial correlation can improve the system performance and thus is an advantage, which is contrary to the traditional point of view. Compared to the Rayleigh fading environments, deployment of large scale antenna arrays in Rician fading environments would be more suitable. For instance, massive MIMO can be applied in microwave backhaul links [26].

Author Contributions: Formal Analysis, Q.Y.; Validation, Y.S.; Writing—Original Draft Preparation, Q.Y., Y.S.; Writing—Review and Editing, D.-W.Y.; Supervision, D.-W.Y.

Funding: This research was funded by the open research fund of State Key Laboratory of Integrated Services Networks, the Fundamental Research Funds for the Central Universities Grant No. 3132016347, and the Natural Science Foundation of Liaoning Province Grant No. 201602086.

Conflicts of Interest: The authors declare no conflict of interest.

References

1. Shafi, M.; Molisch, A.F.; Smith, P.J.; Haustein, T.; Zhu, P.; Silva, P.D.; Tufvesson, F.; Benjebbour, A.; Wunder, G. 5G: A tutorial overview of standards, trials, challenges, deployment, and practice. *IEEE J. Sel. Areas Commun.* **2017**, *35*, 1201–1221. [[CrossRef](#)]
2. Marzetta, T.L. Noncooperative cellular wireless with unlimited numbers of base station antennas. *IEEE Trans. Wirel. Commun.* **2010**, *9*, 3590–3600. [[CrossRef](#)]
3. Ngo, H.Q.; Larsson, E.G.; Marzetta, T.L. Energy and spectral efficiency of very large multiuser MIMO systems. *IEEE Trans. Commun.* **2013**, *61*, 1436–1449.
4. Liu, W.; Han, S.; Yang, C. Energy efficiency scaling law of massive MIMO systems. *IEEE Trans. Commun.* **2017**, *65*, 107–121. [[CrossRef](#)]
5. Yang, H.; Marzetta, T.L. Performance of conjugate and zero-forcing beamforming in large-scale antenna systems. *IEEE J. Sel. Areas Commun.* **2013**, *31*, 172–179. [[CrossRef](#)]
6. Zhang, Q.; Jin, S.; Wong, K.-K.; Zhu, H.; Matthaiou, M. Power scaling of uplink massive MIMO systems with arbitrary-rank channel means. *IEEE J. Sel. Top. Signal Process.* **2014**, *62*, 966–981. [[CrossRef](#)]
7. Rana, M.M.; Kim, J. *Fundamentals of Channel Estimations for Mobile Communications-Existing and New Techniques of a LTE SC-FDMA System*; LAMBERT Academic Publishing: Saarbrücken, Germany, 2012; ISBN 978-3-8454-3137-6.
8. Rusek, F.; Persson, D.; Lau, B.K.; Larsson, E.G.; Marzetta, T.L.; Edfors, O.; Tufvesson, F. Scaling up MIMO: Opportunities and challenges with very large arrays. *IEEE Signal Proc. Mag.* **2013**, *30*, 40–60. [[CrossRef](#)]
9. Yue, D.-W.; Zhang, Y.; Jia, Y.-N. Beamforming based on specular component for massive MIMO systems in Rician fading. *IEEE Wirel. Commun. Lett.* **2015**, *4*, 197–200. [[CrossRef](#)]
10. Yue, D.-W.; Yan, Q. Beamforming only based on specular component for downlink massive MIMO systems. *Wirel. Pers. Commun.* **2017**, *95*, 1799–1810. [[CrossRef](#)]
11. Yue, D.-W.; Meng, Z. LOS component-based equal gain combining for Rician links in uplink massive MIMO. In Proceedings of the 2016 Sixth International Conference on Instrumentation & Measurement, Computer, Communication and Control (IMCCC), Harbin, China, 21–23 July 2016; pp.476–481.
12. Yue, D.-W.; Zhang, Q.T. Generic approach to the performance analysis of correlated transmit/receive diversity MIMO systems with/without co-channel interference. *IEEE Trans. Inf. Theory* **2010**, *56*, 1147–1157. [[CrossRef](#)]
13. Yue, D.-W. Specular component-based beamforming for broadband massive MIMO systems with doubly-ended correlation. *Electron. Lett.* **2016**, *52*, 1082–1084. [[CrossRef](#)]
14. McKay, M.R.; Collings, I.B. On the capacity of frequency-flat and frequency-selective Rician MIMO channels with single-ended correlation. *IEEE Trans. Wirel. Commun.* **2006**, *5*, 2038–2043. [[CrossRef](#)]
15. Dinis, R.; Montezuma, P. Iterative receiver based on the EGC for massive MIMO schemes using SC-FDE modulations. *Electron. Lett.* **2016**, *52*, 972–974. [[CrossRef](#)]
16. Love, D.J.; Heath, R.W. Equal gain transmission in multiple-input multiple-output wireless systems. *IEEE Trans. Commun.* **2003**, *51*, 1102–1110. [[CrossRef](#)]
17. Zheng, X.; Xie, Y.; Li, J.; Stoica, P. MIMO transmit beamforming under uniform elemental power constraint. *IEEE Trans. Signal Process.* **2007**, *55*, 5395–5406. [[CrossRef](#)]

18. Fu, H.; Crussière, M.; H elard, M. BER analysis for equal gain transmission in downlink multiuser MIMO systems. *IEEE Wirel. Commun. Lett.* **2015**, *4*, 533–536. [[CrossRef](#)]
19. Jin, S.; Gao, X.; You, X. On the ergodic capacity of rank-1 Ricean fading MIMO channels. *IEEE Trans. Inf. Theory* **2003**, *53*, 502–517. [[CrossRef](#)]
20. B olskei, H.; Borgmann, M.; Paulraj, A.J. Impact of the propagation environment on the the performance of space-frequency coded MIMO-OFDM. *IEEE J. Sel. Areas Commun.* **2003**, *21*, 427–439. [[CrossRef](#)]
21. Chen, J. When does asymptotic orthogonality exist for very large arrays? In Proceedings of the Global Communications Conference (GLOBECOM), Atlanta, GA, USA, 9–13 December 2013; pp. 4251–4255.
22. Tulino, A.M.; Verdu, S. Random matrix theory and wireless communications. Found. *Trends Commun. Inf. Theory* **2004**, *1*, 1–182. [[CrossRef](#)]
23. Wang, C.-X.; Ge, X.; Cheng, X.; Zhang, G.; Thompson, J. Cooperative MIMO channel models: A survey. *IEEE Commun. Mag.* **2010**, *48*, 80–87. [[CrossRef](#)]
24. Ngo, H.Q.; Suraweera, H.A.; Matthaiou, M.; Larsson, E.G. Multipair full-duplex relaying with massive arrays and linear processing. *IEEE J. Sel. Areas Commun.* **2014**, *32*, 1721–1736. [[CrossRef](#)]
25. Suraweera, H.A.; Krikidis, I.; Yuen, C. Antenna selection in the full-duplex multi-antenna relay channel. In Proceedings of the 2013 IEEE International Conference on Communications (ICC), Budapest, Hungary, 9–13 June 2013; pp. 4823–4828.
26. Durisi, G.; Tarable, A.; Camarda, C.; Devassy, R.; Montorsi, G. Capacity bounds for MIMO microwave backhaul links affected by phase noise. *IEEE Trans. Commun.* **2014**, *62*, 920–929. [[CrossRef](#)]



  2019 by the authors. Licensee MDPI, Basel, Switzerland. This article is an open access article distributed under the terms and conditions of the Creative Commons Attribution (CC BY) license (<http://creativecommons.org/licenses/by/4.0/>).